

**Folic acid conjugated magnetic iron oxide nanoparticles for
nondestructive separation and detection of ovarian cancer
cells from whole blood**

Journal:	<i>Biomaterials Science</i>
Manuscript ID	BM-ART-06-2015-000207.R2
Article Type:	Paper
Date Submitted by the Author:	18-Sep-2015
Complete List of Authors:	Liu, Wenting; The Second Affiliated Hospital to Nanchang University, Nie, Liju; The Second Affiliated Hospital to Nanchang University, Li, Fulai; State Key Laboratory of Food Science and Technology, Nanchang University, Aguilar, Zoraida P.; Ocean Nano Tech, LLC, Xu, Hong; Ocean Nano Tech, LLC, Xiong, YH; Nanchang University, Sino-German Joint Research Institute; Fu, Fen; The Second Affiliated Hospital of Nanchang University, Xu, Hengyi; State Key Laboratory of Food Science and Technology, Nanchang University,

1 **Folic acid conjugated magnetic iron oxide nanoparticles for nondestructive**
2 **separation and detection of ovarian cancer cells from whole blood**

3

4 Wenting Liu^{1,2#}, Liju Nie^{1,2#}, Fulai Li², Zoraida P. Aguilar³, Hong Xu³, Yonghua
5 Xiong², Fu Fen^{1*}, Hengyi Xu^{2*}

6

7 # Co-first authors.

8 1 The Second Affiliated Hospital to Nanchang University, Nanchang 330006, China

9 2 State Key Laboratory of Food Science and Technology, Nanchang University,
10 Nanchang 330047, China

11 3 Ocean NanoTech, LLC., Springdale AR72764, USA

12 *Correspondence to:

13 **Dr. Hengyi Xu**, State Key Laboratory of Food Science and Technology, Nanchang
14 University

15 Address: 235 Nanjing East Road, Nanchang 330047, P.R. China

16 Phone: +0086-791-8830-4447-ext-9512. Fax: +0086-791-8830-4400.

17 E-mail: kidyxu@163.com, HengyiXu@ncu.edu.cn.

18 **Dr. Fen Fu**, The Second Affiliated Hospital to Nanchang University

19 Address: 1 Mingde Road, Nanchang 330006, P.R. China

20 Phone: +0086-791-8671-6961.

21 E-mail: fu_fen@163.com.

22

23 **Abstract**

24 Because of lacking early screening strategies, ovarian cancer is the most deadly
25 cause of gynecologic malignancies. This paper describes an effective method for
26 separation and detection of ovarian cancer cells from female whole blood, using folic
27 acid (FA) conjugated magnetic iron oxide nanoparticles (IO-FA nanoparticles). The
28 IO nanoparticles were synthesized by thermal decomposition and then covalently
29 conjugated with FA. The IO-FA nanoparticles were stably attached to the surface of
30 ovarian cancer cells by coupling to the over-expressed folate receptor (FR), thereby
31 making the cells magnetic. These “magnetic cells” were separated from the complex
32 blood matrix without destruction under the magnetic field. The separation efficiency
33 was as high as 61.3% when the abundance of spiked ovarian cancer SKOV3 cells was
34 as low as $5 \times 10^{-5}\%$. We also successfully detected five (5) out of ten (10) metastatic
35 ovarian cancer patients’ whole blood. This study suggested the feasibility for early
36 detecting of metastatic ovarian cancer cells, which may potentially improve the
37 ovarian cancers patients’ overall survival rate for clinical applications.

38 **Keywords:** IO nanoparticles, folic acid, ovarian cancer, cell separation

39

40 1. Introduction

41 Despite advances in chemotherapy and surgery, ovarian cancer (OC) remains a
42 leading cause of death from gynecologic malignancies. A total of 22,240 new OC
43 cases with 14,030 deaths occurred in the United States in 2013^[1]. When diagnosed in
44 stage I, the 5-year survival rate of women undergoing therapy can reach up to 90%^[2].
45 Unfortunately, over three-quarters of the diagnoses are confirmed with regional or
46 distant metastases due to the absence of specific early warning signs. Early detection
47 of OC is still a huge challenge for clinical workers. Because the ovary is located deep
48 into the pelvic and cannot be felt easily from the outside, there are only a few specific
49 symptoms for OC which are not obvious. In addition, there are many limitations of
50 existing clinical detection methods that tend to lead to misdiagnosis. For example,
51 routine gynecological examination is insensitive when it comes to early cancer
52 detection^[3]. Common clinical imaging modalities, including ultrasound imaging,
53 magnetic resonance imaging (MRI) as well as the electronic computer X-ray
54 tomography imaging (CT) are also insensitive in detecting tumors and metastases that
55 are smaller than 0.5 cm and are incapable of distinguishing between benign and
56 malignancy tumors^[4]. Serum markers such as cancer antigen 125 (CA125) are of
57 limited effectiveness for early detection. For example, CA125 elevated in patients
58 with endometriosis, other diseases or benign conditions, and the baseline expressions
59 are widely different^[5]. Thus, there is a significant need for effective early screening
60 strategy to reduce OC recurrence probability and mortality.

61 Previous researches showed that circulating tumor cells (CTCs) in the peripheral

62 blood of patients originated from early or metastatic tumors, which could present a
63 window for early detection of asymptomatic OC^[6-8]. The detection of CTCs could
64 provide a sensitive and minimally invasive way for early diagnosis and prognosis
65 evaluation, especially when the primary tumor is difficult to detect with currently
66 available methods. However, the concentration of CTCs is extremely low, ranging
67 from 1 per billion to 1 per 10,000,000 nucleated blood cells. Hence, various
68 techniques have been explored for capture, enrichment, and detection of CTCs^[9-13].
69 The current common clinical CTCs enrichment procedures are filtration,
70 immunomagnetic procedures with antibodies against either common leukocyte
71 antigen CD45 (negative selection) or the tumor-associated antigens (positive selection)
72 and density gradient centrifugation^[7]. However, most of these methods are limited by
73 their slow separation rates or the requirement for complicated pre-treatment. These
74 limitations may damage the rare CTCs and make them more difficult to detect. So far,
75 approaches to detect CTCs can be classified into PCR-based and cytometric methods.
76 PCR-based methods have a high false-positive rate because the high sensitivity not
77 only reveal the specific genes of cancer cells but also the expression of illegitimate
78 transcripts in peripheral-blood leukocytes, the presence of mRNA in normal cells
79 circulating at a low frequency, or contamination in blood samples during venipuncture.
80 It is also error-prone for low-quality samples (one tumor cell usually contains only a
81 single copy of the target gene)^[14]. Common cytometric methods such as
82 immunocytochemistry and fluorescence-activated flow cytometry have been widely
83 used on samples, but it may lead to a high rate of false-negative because of the need

84 for specific antibodies and the elimination of interferences. As a result, enrichment
85 and detection of rare CTCs in patients' peripheral whole blood remains a technical
86 challenge^[6].

87 Magnetic iron oxide (IO) nanoparticles have promising potentials in the isolation and
88 detection of trace amounts of analytes because of their high surface-to-volume ratio,
89 excellent enrichment capability, and biocompatibility^[15] which potentially allows
90 highly efficient non-destructive analyte isolation. In this research, we demonstrated an
91 effective method to separate and detect circulating OC cells from patients' whole
92 blood using IO-folic acid (IO-FA) nanoparticles under a low magnetic field gradient.

93 The small size IO nanoparticle (25 nm) was able to contact with the surface of the
94 cells more efficiently and prevent the cells from tearing into pieces at the time of
95 separation. The IO nanoparticles were synthesized by a pyrolysis-based method and
96 coated with polymers to obtain the water soluble and biocompatible form. For cell
97 capture, the IO nanoparticles were modified with FA which was used as a targeting
98 ligand for OC cells that are rich in FR. When compared with antibodies (eg. EpCAM),
99 FA has many advantages: 1) FA (vitamin B₉) is essential for the eukaryotic cell in the
100 nuclear glucoside synthesis as one-carbon donors. Moreover, it is a co-enzyme for the
101 DNA synthesis and is utilized by various enzymatic systems^[16, 17]. Therefore, FA is
102 less immunogenic and safe enough for use in the human body. 2) The expression of
103 folate receptor (FR), especially FR α , is much higher in many epithelial tumors
104 relative to normal tissues. It was reported that 90% of OC solid tumors over expressed
105 FR^[18]; 3) FA has a high affinity ligand for the FR ($K_d = 0.1\text{nM}$)[19], so that IO-FA

106 nanoparticles could bind to FR found on cell surfaces efficiently and stably; 4) It is
107 cost-effective and easy to store. In addition, the specificity of the IO-FA nanoparticles
108 for targeting OC cells was successfully monitored by Prussian blue staining.
109 Furthermore, IO-FA nanoparticles showed outstanding capture efficiency for OC cells
110 in female fresh whole blood without any pre-treatment process. Finally, the
111 identification and characterization of OC cells involved an extremely sensitive and
112 specific analysis. Human epididymis protein 4 (HE4) has been illustrated to be
113 over-expressed in OC cells and exhibits an advantage over the CA125 assay because
114 it is less frequently positive in patients with other diseases ^[20, 21]. Thus, the isolated
115 OC cells were identified with a simple QD-based immunofluorescence staining using
116 the OC specific marker HE4. The scheme for OC cells separation and detection from
117 the whole blood is shown in Fig.1.

118 **2. Materials and methods**

119 **2.1 Materials**

120 SKOV3, OC cell line with FR-positive cell surface were gifted from the Medical
121 Research Center of the First Affiliated Hospital to Nanchang University. Lung cancer
122 A549 cell lines with FR-negative cell surface were gifted from Jiangxi academy of
123 medical science[22]. OC patients and normal female whole blood containing
124 ethylenediaminetetraacetic acid (EDTA) as anticoagulant were obtained from the First
125 Affiliated Hospital to Nanchang University, the Second Affiliated Hospital to
126 Nanchang University, Jiangxi maternal and child health hospital, and Jiangxi
127 Provincial Cancer Hospital. Albumin bovine V (BSA) was purchased from
128 BIOSHARP (Hefei, China). Folate-free RPMI 1640 culture media was purchased
129 from GIBCO (Grand Island, NY). The fetal bovine serum (FBS) and trypsin were
130 from Trans Gen Biotech (Beijing, China). Goat polyclonal anti-HE4 (C-12) was
131 purchased from Santa Cruz Biotechnology, Inc. (Dallas, TX). Fluorescein
132 isothiocyanate (FITC) conjugated AffiniPure Rabbit Anti-goat IgG was from EarthOx
133 LLC (Millbrae, CA). All other chemicals of analytical grade were provided by
134 SangonBiotech (Shanghai, China).

135 **2.2 Synthesis of IO nanoparticles**

136 The IO nanoparticles were synthesized by thermal decomposition following the
137 experimental procedures reported elsewhere with iron oxide powder as the iron
138 precursor, oleic acid as the ligands, and octadecene as the solvent^[23]. These
139 hydrophobic IO nanoparticles were coated with amphiphilic polymers as reported

140 previously^[24]. In brief, a polymer/IO ratio of 5-10 was used, after vacuum drying, the
141 encapsulated IO nanoparticles were suspended in a polar solvent (aqueous buffer) and
142 then purified.

143 **2.3 Conjugation of IO nanoparticles with FA**

144 Before conjugation with the IO nanoparticles, FA was first conjugated to diamine
145 PEG (polyethylene glycol, PEG) to increase the flexibility of FA for optimal
146 recognition between FA and its receptor, FR, and offer the amine group (-NH₂) to
147 covalently attach to the carboxyl group (-COOH) on the IO nanoparticles. In brief,
148 100 mg of FA in 10 mL dimethylsulfoxide (DMSO) was activated with 50 mg of
149 dicyclohexylcarbodiimide (DCC) in the presence of 1 mL of triethylamine and 50 mg
150 of N-hydroxysuccinimide (NHS) at room temperature in the dark for 4 hours, in
151 which 0.5 g of diamine PEG was added to achieve the FA/DCC/NHS/PEG ratio of
152 1/1.1/1.1/1. This reaction continued overnight at room temperature in the dark. The
153 by-product of this reaction, dicyclohexylurea was removed by centrifugation at 4,000
154 rpm for 5 min. For purification, 10 times volume of cold acetone (-20°C) was added
155 to the reaction mixture to precipitate the FA-PEG-NH₂. The FA-PEG-NH₂ was
156 collected by centrifugation at 4,000 rpm for 15 min and the pellet was washed three
157 times with ethyl acetate. The pellet was dried in the fume hood and stored in the dark.

158 The FA-PEG-NH₂ was conjugated to the IO nanoparticles in the following manner:
159 1 mg of 25 nm IO nanoparticles dissolved in 0.5 mL borate buffer (200 mM, pH=7)
160 was activated with 0.2 mg of
161 1-Ethyl-3-[3-dimethylaminopropyl]carbodiimidehydrochloride (EDC) and 0.1 mg

162 NHS, after which 7 mg of FA-PEG-NH₂ dissolved in 0.5 mL borate buffer (200 mM,
163 pH=7) was added. The reaction was incubated at room temperature for 2 hours with
164 continuously stirring. The resulting IO-PEG-FA (or simply, IO-FA) nanoparticles
165 were purified using a magnetic separator with magnetic field gradient of 1.0 T.

166 **2.4 Characterization of IO-FA and IO nanoparticles**

167 The shape and size of the IO nanoparticles were observed under transmission
168 electron microscopy (TEM). The hydrodynamic diameter and the zeta potential of the
169 IO and IO-FA in ultrapure water were measured using Laser particle size analyzer
170 (Malvern, England). For the IO nanoparticles gel electrophoresis, 1% (w/v) agarose
171 gel in 0.5×TBE buffer system was ran at a voltage of 90 V for 15 min and 20%
172 glycerol was mixed with samples before loading. Fourier Transform infrared
173 spectroscopy (FTIR) (Thermo Nicolet, USA) was used to confirm the covalent bond.

174 **2.5 Cell culture**

175 SKOV3 cells and A549 cells were cultured in culture flasks that contained 15 mL
176 folate-free RPMI-1640 medium supplemented with 10% FBS in a humidified 5% CO₂
177 atmosphere at 37°C. When cells became 80% confluent, they were detached from the
178 cell culture flask with trypsin and rinsed once with PBS. The cells were harvested by
179 centrifugation at 1000 rpm for 1 min and the cell pellet was re-suspended in PBS
180 before storage at 4°C.

181 **2.6 Specificity test of IO-FA nanoparticles by Prussian blue staining**

182 SKOV3 cells and A549 cell lines, with 80% confluence were respectively detached
183 and harvested with centrifugation at 1000 rpm for 1 min. The cell pellet was

184 re-suspended in 90 μ L PBS after washed once with PBS. Two aliquot number of cells
185 were separately incubated with 50 μ L IO nanoparticles and IO-FA nanoparticles at
186 room temperature for 2 hours and washed twice with PBS, respectively. The cells
187 were recovered by centrifugation and re-suspended in 25 μ L PBS. To these, 25 μ L
188 freshly prepared Prussian blue stain solution (1:1 mixture of 10% potassium
189 ferrocyanide (II) trihydrate and 20% HCl) was added. The cell-Prussian blue mixture
190 was incubated at 37°C for 30 min and the stained cells were washed once with PBS
191 before observation under a microscope.

192 **2.7 Separation of spiked OC cells from whole blood using IO-FA nanoparticles**

193 The whole blood from healthy female volunteers were spiked with SKOV3 cells at
194 about 450 cells/mL. The cultured cells were pre-stained with fluorescent dye
195 Hoechst33342 and counted as follows: Hoechst33342 stain was added into the
196 SKOV3 cells at a concentration of 1 μ L/mL. After incubation for 30 min, the cells
197 were washed three times with PBS and counted using a hemocytometer^[25]. A 100 μ g
198 aliquot of IO-FA nanoparticles was mixed with the spiked blood (1 mL) at room
199 temperature for 2 h, which were then placed on a magnetic separator with a magnetic
200 strength of 1.0 T for 4h. The blood was pipetted out carefully, and the pellet
201 containing IO-FA nanoparticles captured cells was re-suspended in 25 μ L PBS for cell
202 counting under a fluorescence microscope. Wright's stain was used to inspect and
203 identify the captured cells from the whole blood in a strong magnetic field following
204 the manufacturer's protocol. The number of SKOV3 cells spiked in the whole blood
205 was extremely small compared with the cell population in human whole blood. After

206 application of the Wright's stain, the samples were smeared on a slide and observed
207 using the oil immersion lens of the microscope. Moreover, a recovery test has been
208 performed using 1 mL normal human whole blood spiked with SKOV3 (19.5 ± 2.5 ,
209 67.5 ± 7.5 , 143 ± 45 , 243 ± 11.5 , 305 ± 9.0 cells), and each recovery has been calculated.

210 **2.8 Detection of OC cells**

211 In order to test the ability of our method in detecting OC cells in patients' whole
212 blood, a total of 10 metastatic OC patients' whole blood (serous or endometrioid
213 ovarian carcinomas) without any pre-treatment were chosen and subjected to the
214 IO-FA protocol. After isolated from the blood and re-suspension as above, the cells
215 were smeared, dried, and fixed with methanol at -10°C . The fixed cells were blocked
216 with 5% BSA in PBS and washed after 20 min. The isolated cells were incubated with
217 anti-HE4 (1:50 diluted in PBS) for 60 min, washed three times with PBS, and
218 incubated with FITC-AffiniPure Rabbit Anti-goat IgG(1:100 diluted in PBS) for 30
219 min and observed under a fluorescence microscope after being mounted with 90%
220 glycerol in PBS.

221 **2.9 Statistical analysis**

222 All statistical analysis was performed using SPSS 17.0 software. All tests were
223 repeated independently in triplicates.

224

225 3. Results and discussion

226 3.1. Characterization of IO and IO-FA nanoparticles

227 IO nanoparticles were successfully synthesized by thermal decomposition method.
228 Since IO nanoparticles are hydrophobic, an amphiphilic polymer was coated to
229 convert into the biocompatible water soluble form, which can be easily conjugated
230 with proteins, peptides or other amine-containing molecules^[26]. The IO nanoparticles
231 were characterized in terms of their size and monodispersity before use. The TEM
232 images of the IO nanoparticles coated with amphiphilic polymer (Fig. 2A), showed
233 that the particles were spherical with an average inorganic core of 25 nm in diameter.
234 The DLS images (Figs. 2B and 2C) showed the change in the IO nanoparticles size
235 before and after conjugation with FA. After formation of the IO-FA, the IO
236 nanoparticles showed an increased hydrodynamic size, but the increase was not
237 significant due to the low molecular weight of FA-PEG-NH₂. The zeta potential of the
238 IO-FA nanoparticles increased to -32.6 mV compared with the IO before conjugation
239 which was -51.1 mV (Fig. 2C). This may be attributed to the decrease in the exposed
240 negative carboxyl groups which reacted with the FA-PEG-NH₂ during conjugation.
241 The change in molecular mobility of the IO nanoparticles before and after conjugation
242 with FA was also demonstrated on the gel electrophoresis (Fig. 2D). The IO-FA
243 nanoparticles moved slower than IO nanoparticles, indicating a higher molecular
244 weight and a less negative zeta potential. The conjugation of FA with IO nanoparticles
245 was further confirmed by FTIR (Fig. 2E). The FTIR absorbance vibrational peak at 541
246 cm⁻¹ in both IO and IO-FA spectra corresponded to the Fe-O bond, while significant

247 peaks at 1178 cm^{-1} , 1623 cm^{-1} and 3400 cm^{-1} in the IO-FA spectrum may be attributed
248 to C-N stretch, C=O stretch and N-H stretch from the amide linkage formed between
249 the FA-PEG-NH₂ and IO nanoparticles. Furthermore, the peaks at 1623 cm^{-1} and 1430
250 cm^{-1} in the FTIR of IO-FA spectrum also corresponded to the aromatic ring stretch of
251 the pteridine ring and p-amino benzoic acid moieties of FA^[27]. These results revealed
252 that the FA-PEG-NH₂ was bound on the surface of the IO nanoparticles successfully.

253 **3.2 IO-FA nanoparticles specifically attached to the SKOV3 cells**

254 In order to demonstrate the specificity of the IO-FA nanoparticles
255 for capturing SKOV3 cells, prussian blue staining was used which reacts with the iron.
256 When IO-FA nanoparticles attached to the surface of SKOV3 cell successfully, the
257 potassium ferrocyanide ($\text{K}_4\text{Fe}(\text{CN})_6$) reacts with the iron ion from the IO
258 nanoparticles and form ferrous ferricyanide ($\text{Fe}_4[\text{Fe}(\text{CN})_6]_3$) which appears as a dark
259 blue coloration. The control group composed of A549 cell lines which do not express
260 FR and IO-nanoparticles without conjugated FA were also subjected to the same tests.
261 As shown in Fig.3A, SKOV3 cells incubated with IO-FA nanoparticles were
262 specifically labeled blue while SKOV3 cells incubated with IO nanoparticles without
263 FA, A549 cells that lack FR incubated with IO-FA nanoparticles, or A549 cells
264 incubated with IO nanoparticles, showed insignificant blue coloration (Figs. 3B, 3C
265 and 3D, respectively). These results indicated that IO-FA nanoparticles were
266 specifically attached to the SKOV3 cells through the FA-FR interaction with minimal
267 to no non-specific interaction.

268 **3.3 Selective capture of spiked OC cells from whole blood using IO-FA**

269 **nanoparticles**

270 To evaluate the efficiency of these IO-FA nanoparticles in the selective capture of
271 OC CTCs, enrichment experiments were carried out using whole blood spiked with
272 SKOV3 cells. In order to identify the SKOV3 cells from the cells in the blood matrix,
273 SKOV3 cells were pre-stained with the fluorescent dye Hoechst33342. As shown in
274 Figs. 4A and 4B, SKOV3 cells were stained well and had a long-term stability and
275 brightness. Blood, a complex medium containing a variety of cells and components
276 including billions of red blood cells and white blood cells, has an average number of
277 white blood cells in healthy women's whole blood at $(4-10) \times 10^9$ cells/L and red blood
278 cells at $(3.5-5) \times 10^{12}$ cells/L. In order to replicate the CTCs in human blood circulation
279 system, 450 cancer cells were mixed with 1 mL of whole blood sample from women
280 at a ratio of about 1:10,000,000. IO-FA nanoparticles were added to selectively
281 capture the spiked SKOV3 cells. As shown in Fig.4C, SKOV3 cells were successfully
282 captured from the whole blood, and were easily identified with strong blue
283 fluorescence under a fluorescence microscope. The efficiency of these IO-FA
284 nanoparticles in the selective separation of the spiked SKOV3 cells ranged from
285 52.3% to 68.3% (N=4), with an average of 61.3% (Fig.4D). The results clearly
286 indicated the promising capabilities of the IO-FA nanoparticles in enriching OC cells
287 with high levels of FR expression from whole blood. Also, the feasibility of the
288 method for using FA coated MNPs to enrich and detect CTCs from whole blood was
289 confirmed with the recovery test, and results showed 42.66% to 65.18% recovery with
290 19.5 ± 2.5 to 305 ± 9.0 cells per mL.

291 In order to identify and observe the morphological changes of these cancer cells after
292 magnetic separation from whole blood, Wright's stain was used. Wright's stain is
293 commonly used in clinical practice to reveal the cell structure and to distinguish
294 different types of cells. Cultured SKOV3 cells stained with Wright stain were big in
295 size with a large, irregular, and hyperchromatic nucleus (Fig.4E). The morphology of
296 SKOV3 cells were very different from the blood cells, after isolated by IO-FA
297 nanoparticles with the magnet, the captured cells were intact and the same as
298 cultured (Fig.4F). These results indicated that the IO-FA nanoparticles specifically
299 bound to the SKOV3 cells through the FA-FR interaction, which rendered the cells
300 magnetic without visible morphological damage. Therefore, it may be feasible to
301 effectively capture and detect cancer cells from circulation in peripheral blood for
302 early diagnosis of OC.

303 **3.4 Detection of OC cells in peripheral blood of patients with metastatic OC**

304 In order to test the ability of the IO-FA method in isolating OC cells in patients'
305 whole blood, a total of 10 metastatic OC patients' whole blood (serous or
306 endometrioid ovarian carcinomas) without any pre-treatment were used.
307 Immunofluorescence staining was used to confirm the capture of the OC cells through
308 the biomarker HE4 which is a widely recognized tumor marker that is over-expressed
309 in OC cells, especially in serous and endometrioid ovarian carcinomas^[28]. The OC
310 cells were fluorescent green and bigger in size than the blood cells under the
311 fluorescence microscope as shown in Fig. 5. The results indicated successful detection
312 of the OC cells in 5 samples from 10 metastatic OC patients' whole blood. However,

313 further studies must be carried out to improve the recovery, efficiency, and accuracy

314 of the chosen detection method.

315

316 4. Conclusion

317 Early diagnosis of OC remains a problem for clinical treatment. Although magnetic
318 nanomaterials have been widely used in the detection of tumor cells, which holds
319 promise for early diagnosis of OC, separating cancer cells from the whole blood
320 directly still faces a lot of difficulties such as low separation efficiency, process
321 complexity, and pre-treatment requirement (thinning the blood or incubating cancer
322 cells with magnetic nanoparticles of various sizes)^[29-32]. In this report, we
323 demonstrated the feasibility of using 25nm IO-FA nanoparticles for nondestructive
324 OC cell enrichment and detection from whole blood. After conjugated with FA, the IO
325 nanoparticles attached to the surface of OC cells efficiently and securely, allowing
326 separation from the complex human whole blood without destructive effect to the cell
327 morphology with the use of a strong magnetic field. The separation efficiency was as
328 high as 61.3% when the abundance of cancer cells was as low as 450 cells in 1 mL of
329 blood which translates to $5 \times 10^{-5}\%$ CTCs in whole blood, which was much higher
330 than other published methods^[30, 32]. Out of 10 metastatic OC patients' whole blood,
331 cancer cells were successfully detected in 5 samples by the new IO-FA method. The
332 results of this study suggested the feasibility of using IO-FA nanoparticles for
333 isolation of CTCs for the early detection of metastatic OC.

334 **Acknowledgments**

335 This project was supported by National Natural Science Foundation of China
336 (81201691 and 31271863), Science and Technology Planning Project of Jiangxi
337 Province (20151BBG70077), research fund for the Doctoral Program of Higher
338 Education of China (20123601120005), and Training Plan for the Young Scientist
339 (Jinggang Star) of Jiangxi Province (20142BCB23004).

340

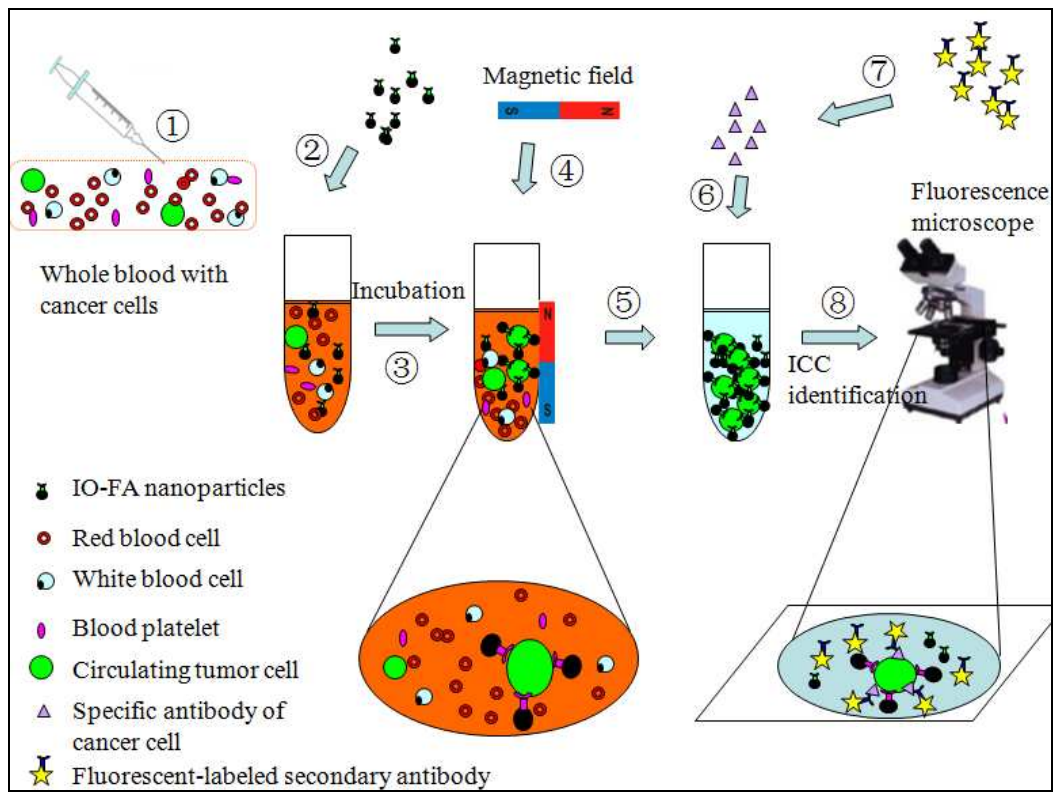
341 **References**

- 342 1. Siegel, R., D. Naishadham, and A. Jemal, *Cancer statistics, 2013*. CA: a cancer journal for
343 clinicians, 2013. **63**(1): p. 11-30.
- 344 2. Badgwell, D. and R.C. Bast Jr, *Early detection of ovarian cancer*. Disease markers, 2007.
345 **23**(5): p. 397-410.
- 346 3. Das, P.M. and R.C. Bast Jr, *Early detection of ovarian cancer*. 2008.
- 347 4. Popovtzer, R., et al., *Targeted gold nanoparticles enable molecular CT imaging of cancer*.
348 Nano letters, 2008. **8**(12): p. 4593.
- 349 5. Choi, Y.-E., J.-W. Kwak, and J.W. Park, *Nanotechnology for early cancer detection*. Sensors,
350 2010. **10**(1): p. 428-455.
- 351 6. Joseph, L., *Circulating Tumor Cells and Nucleic Acids for Tumor Diagnosis*, in *Molecular*
352 *Pathology of Neoplastic Gastrointestinal Diseases* 2013, Springer. p. 229-247.
- 353 7. Pantel, K. and C. Alix-Panabières, *Circulating tumour cells in cancer patients: challenges and*
354 *perspectives*. Trends in molecular medicine, 2010. **16**(9): p. 398-406.
- 355 8. Yu, M., et al., *Circulating tumor cells: approaches to isolation and characterization*. The
356 Journal of cell biology, 2011. **192**(3): p. 373-382.
- 357 9. Racila, E., et al., *Detection and characterization of carcinoma cells in the blood*. Proceedings
358 of the National Academy of Sciences, 1998. **95**(8): p. 4589-4594.
- 359 10. Scarberry, K.E., et al., *Magnetic nanoparticle-peptide conjugates for in vitro and in vivo*
360 *targeting and extraction of cancer cells*. Journal of the American Chemical Society, 2008.
361 **130**(31): p. 10258-10262.
- 362 11. Adams, A.A., et al., *Highly efficient circulating tumor cell isolation from whole blood and*
363 *label-free enumeration using polymer-based microfluidics with an integrated conductivity*
364 *sensor*. Journal of the American Chemical Society, 2008. **130**(27): p. 8633-8641.
- 365 12. Ntoulia, M., et al., *Detection of Mammaglobin A-mRNA-positive circulating tumor cells in*
366 *peripheral blood of patients with operable breast cancer with nested RT-PCR*. Clinical
367 biochemistry, 2006. **39**(9): p. 879-887.
- 368 13. Ohlmann, C.-H., et al. *Detection of circulating tumor cells in patients with renal cell*
369 *carcinoma by reverse transcriptase polymerase chain reaction for G250/MNCA-9: results of a*
370 *prospective trial*. in *Urologic Oncology: Seminars and Original Investigations*. 2006. Elsevier.
- 371 14. Mocellin, S., et al., *Circulating tumor cells: the 'leukemic phase' of solid cancers*. Trends in
372 molecular medicine, 2006. **12**(3): p. 130-139.
- 373 15. Cohen, Y. and S.Y. Shoushan, *Magnetic nanoparticles-based diagnostics and theranostics*.
374 Current opinion in biotechnology, 2013.
- 375 16. Hong, G., et al., *Folate-functionalized polymeric micelle as hepatic carcinoma-targeted,*
376 *MRI-ultrasensitive delivery system of antitumor drugs*. Biomedical microdevices, 2008. **10**(5):
377 p. 693-700.
- 378 17. Chen, C., et al., *Structural basis for molecular recognition of folic acid by folate receptors*.
379 Nature, 2013.
- 380 18. Low, P.S. and S.A. Kularatne, *Folate-targeted therapeutic and imaging agents for cancer*.
381 Current opinion in chemical biology, 2009. **13**(3): p. 256-262.
- 382 19. Pinhassi, R.I., et al., *Arabinogalactan-Folic Acid-Drug Conjugate for Targeted Delivery*
383 *and Target-Activated Release of Anticancer Drugs to Folate Receptor-Overexpressing*

- 384 *Cells. Biomacromolecules*, 2009. **11**(1): p. 294-303.
- 385 20. Welsh, J.B., et al., *Analysis of gene expression profiles in normal and neoplastic ovarian*
386 *tissue samples identifies candidate molecular markers of epithelial ovarian cancer.*
387 *Proceedings of the National Academy of Sciences*, 2001. **98**(3): p. 1176-1181.
- 388 21. Hellström, I., et al., *The HE4 (WFDC2) protein is a biomarker for ovarian carcinoma.* *Cancer*
389 *research*, 2003. **63**(13): p. 3695-3700.
- 390 22. Zheng, Y., et al., *Preparation and characterization of folate-poly (ethylene*
391 *glycol)-grafted-trimethylchitosan for intracellular transport of protein through folate*
392 *receptor-mediated endocytosis.* *Journal of biotechnology*, 2010. **145**(1): p. 47-53.
- 393 23. William, W.Y., et al., *Synthesis of monodisperse iron oxide nanocrystals by thermal*
394 *decomposition of iron carboxylate salts.* *Chemical Communications*, 2004(20): p. 2306-2307.
- 395 24. Gao, X., et al., *In vivo cancer targeting and imaging with semiconductor quantum dots.*
396 *Nature biotechnology*, 2004. **22**(8): p. 969-976.
- 397 25. Kaittanis, C., S. Santra, and J.M. Perez, *Role of nanoparticle valency in the nondestructive*
398 *magnetic-relaxation-mediated detection and magnetic isolation of cells in complex media.*
399 *Journal of the American Chemical Society*, 2009. **131**(35): p. 12780-12791.
- 400 26. Pellegrino, T., et al., *Hydrophobic nanocrystals coated with an amphiphilic polymer shell: a*
401 *general route to water soluble nanocrystals.* *Nano letters*, 2004. **4**(4): p. 703-707.
- 402 27. Sun, C., R. Sze, and M. Zhang, *Folic acid-PEG conjugated superparamagnetic nanoparticles*
403 *for targeted cellular uptake and detection by MRI.* *Journal of Biomedical Materials Research*
404 *Part A*, 2006. **78**(3): p. 550-557.
- 405 28. Drapkin, R., et al., *Human epididymis protein 4 (HE4) is a secreted glycoprotein that is*
406 *overexpressed by serous and endometrioid ovarian carcinomas.* *Cancer research*, 2005. **65**(6):
407 p. 2162-2169.
- 408 29. Chen, Z., et al., *Graphite-Coated Magnetic Nanoparticle Microarray for Few-Cells*
409 *Enrichment and Detection.* *ACS nano*, 2012. **6**(2): p. 1094-1101.
- 410 30. Hossain, M., et al., *X-ray enabled detection and eradication of circulating tumor cells with*
411 *nanoparticles.* *Biosensors and Bioelectronics*, 2012.
- 412 31. Sha, M.Y., et al., *Surface-enhanced Raman scattering tags for rapid and homogeneous*
413 *detection of circulating tumor cells in the presence of human whole blood.* *Journal of the*
414 *American Chemical Society*, 2008. **130**(51): p. 17214-17215.
- 415 32. Banerjee, S.S., et al., *Transferrin-Mediated Rapid Targeting, Isolation, and Detection of*
416 *Circulating Tumor Cells by Multifunctional Magneto-Dendritic Nanosystem.* *Advanced*
417 *healthcare materials*, 2012.
- 418
- 419

420 **Figures**

421

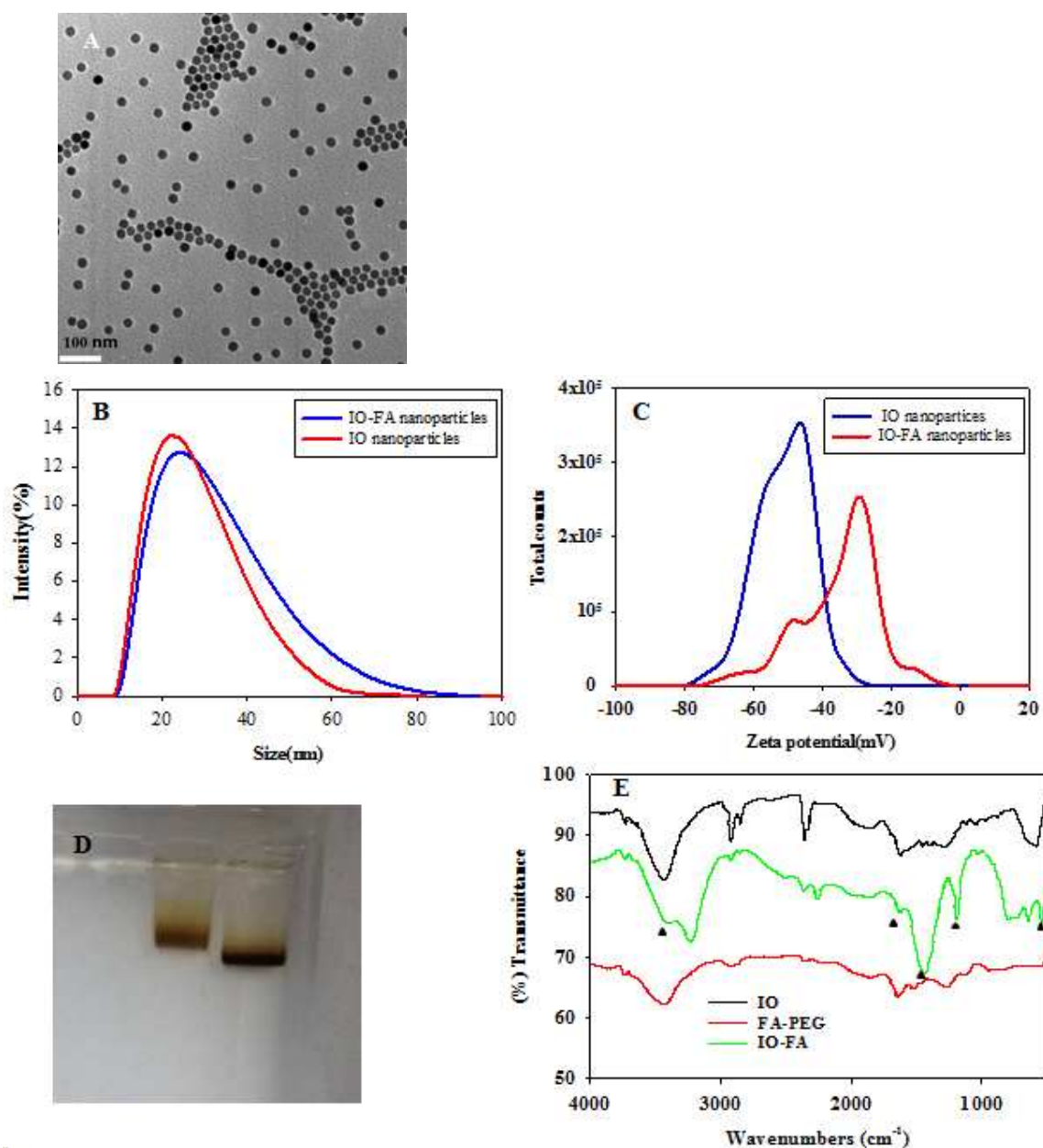


423 **Fig. 1** Testing scheme of OC cells separation and detection from whole blood using

424 IO-FA nanoparticles.

425

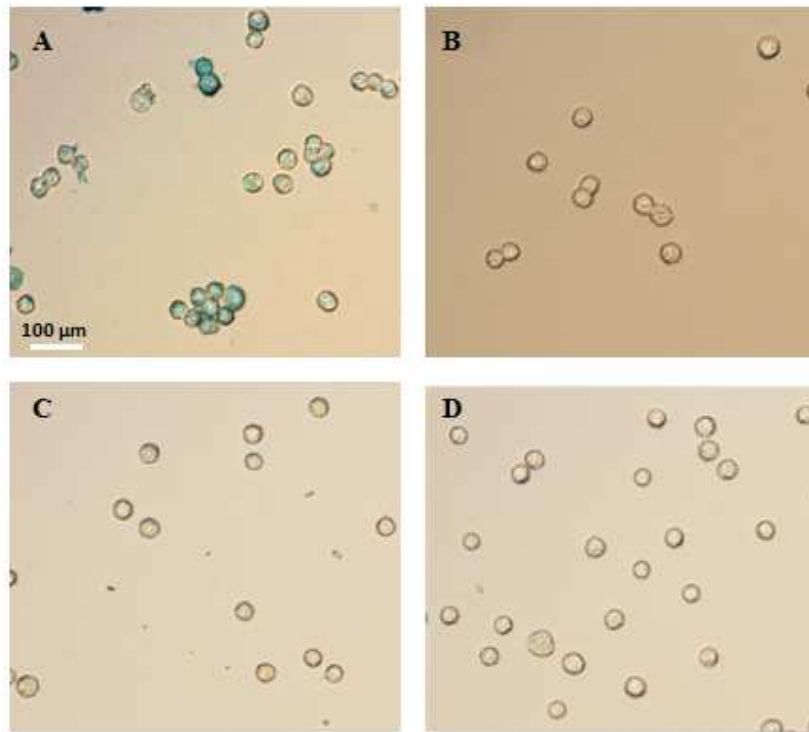
426



427

428 **Fig. 2** Characterizations of IO nanoparticles and IO-FA nanoparticles. (A) TEM
 429 images of synthesized IO nanoparticles coated with amphiphilic polymer; DLS
 430 images of the IO-nanoparticles before/after conjugation with FA shows (B) IO-FA
 431 nanoparticles with a little higher hydrodynamic size than IO nanoparticles, and (C)
 432 IO-FA nanoparticles with a less negative zeta potential than IO nanoparticles; (D)
 433 agarose gel electrophoresis of biocompatible water soluble amphiphilic polymer
 434 coated IO nanoparticles (on right) and IO-FA nanoparticles (on left); (E) FTIR
 435 spectrum of IO nanoparticles, FA-PEG, and IO-FA nanoparticles.

436



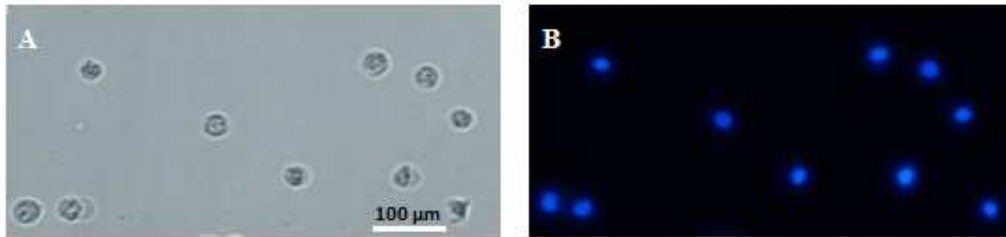
437

438

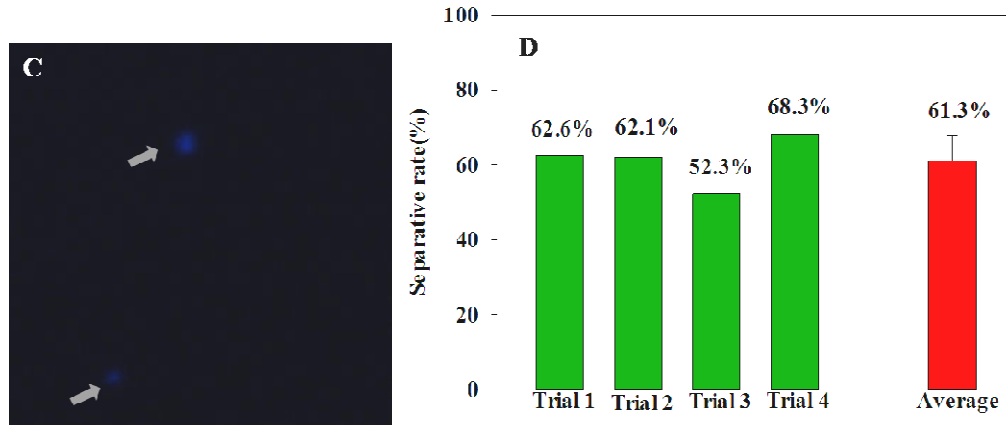
439 **Fig. 3** Cell staining with Prussian blue. (A) SKOV3 cells exposed to IO-FA
440 nanoparticles; (B) SKOV3 cells exposed to IO nanoparticles; (C) A549 cells exposed
441 to IO-FA nanoparticles; (D) A549 cells exposed to IO nanoparticles.

442

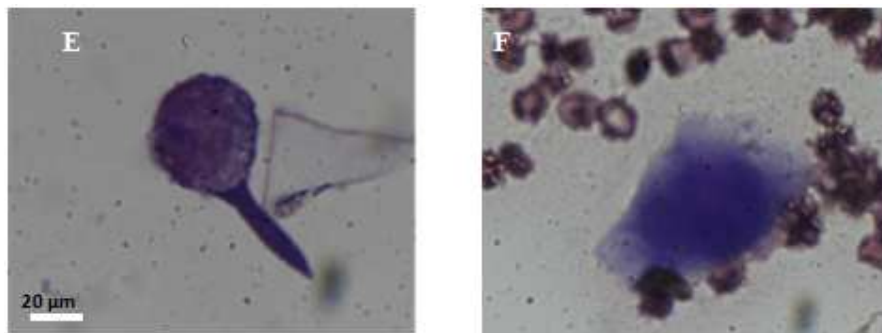
443



444



445



446

447 **Fig. 4** SKOV3 cells separation in spiked female whole blood. Hoechst pre-stained
 448 SKOV3 cells under (A) white light and (B) UV light in PBS of thunder a
 449 fluorescencemicroscope; (C) IO nanoparticles separated Hoechst pre-stained SKOV3
 450 cells from female whole blood under fluorescencemicroscope; (D) The efficiency of
 451 IO-FA nanoparticles capture of SKOV3 cells; (E) SKOV3 cells stained with wright's
 452 stain in PBS and (F) Wright stained IO-FA isolated SKOV3 cells from female whole
 453 blood under the oil immersion lens of the microscope.

454

455



456

457

458 **Fig. 5** Immune fluorescence images of OC cell isolated with the IO-FA from cancer
459 patient's whole blood under a fluorescence microscope.

Graphical abstract

An effective method for separation and detection of ovarian cancer cells from whole blood using folic acid conjugated magnetic nanoparticles.

